NEOPLASMA accepted, ahead of print manuscript
Cite article as https://doi.org/10.4149/neo_2025_241031N442

Running title: HSF1 activates CLDN3 to facilitate CRC progression

Elevated expression of HSF1 promotes the progression of colorectal cancer by activating CLDN3 transcription

Yanxi Shao[1,#], Ting Ma[1,#], Dening Ma[1,2], Lue Hong[3], Min Lv[2], Shiqi Zhou[1], Zhibin Fang[1], Enyan Yu[4], Xia Li[1,5,*], Yuping Zhu[1,2,*]

[1]Postgraduate Training Base Alliance of Wenzhou Medical University, Zhejiang Cancer Hospital, Hangzhou, China; [2]Department of Colorectal Surgery, Zhejiang Cancer Hospital, Hangzhou, China; [3]The First School of Clinical Medicine, Zhejiang Chinese Medical University, Hangzhou, China; [4]Department of Clinical Psychology, Zhejiang Cancer Hospital, Hangzhou, China; [5]Zhejiang Cancer Research Institute, Zhejiang Cancer Hospital, Hangzhou, China

*Correspondence: lixia@zjcc.org.cn; zhuyp@zjcc.org.cn

[#]Contributed equally to this work.

Received October 31, 2024 / Accepted March 10, 2025

Colorectal cancer (CRC) is the most common gastrointestinal malignancy worldwide, with increasing morbidity and mortality. Heat shock transcription factor 1 (HSF1), as an important transcription factor regulating the expression of heat shock proteins, has been proven to play a crucial role in the development of various tumors. Yet the potential mechanism and clinical significance of HSF1 in CRC remain unclear and require further exploration. We used TCGA database to understand the clinical significance of HSF1 in CRC. Then, we verified the expression of HSF1 in CRC tissues by immunohistochemistry and analyzed its clinical significance. By constructing stable knockdown and overexpressed of HSF1 in cell lines to investigate the potential mechanisms of HSF1 to regulate CRC cell proliferation, migration, and invasion *in vivo* and *in vitro*. Next, differential genes expressed by HSF1 in CRC were analyzed by bioinformatics technology, and their correlation and interaction were verified by PCR, WB, and CHIP experiments. We confirmed that HSF1 is highly expressed in CRC and its upregulation is associated with poor prognosis of malignant events in CRC. Functionally, HSF1 can enhance the proliferation, invasion, and migration of CRC cell lines. *In vivo* experiments have shown that knockdown of HSF1 can inhibit tumor growth. In terms of molecular mechanism, we found that HSF1 can directly bind to the transcription factor binding site of CLDN3 and activate its transcription. Our research demonstrates the clinical significance and carcinogenic effect of HSF1. The functional mechanisms of HSF1 and its targets may serve as diagnostic and therapeutic targets for CRC.

Key words: HSF1; CLDN3; progression; colorectal cancer

Colorectal cancer (CRC) is a gastrointestinal malignancy that is widespread worldwide, and both its incidence and mortality have been increasing in recent years [1]. According to the latest Global cancer statistics 2020, CRC is considered the third most frequent cancer globally and ranks second in cancer mortality [2]. Base on the current diagnosis and treatment methods, although the 5-year overall survival (OS) rate for all CRC patients is approximately 65%, the 5-year OS rate for patients with metastatic colorectal cancer (mCRC) in stage IV is only 13% [3, 4]. Hence, it is necessary to understand the mechanism of CRC development to provide new basis for the discovery of treatment and prognostic biomarkers.

Heat shock transcription factor 1 (HSF1) is the primary member of the heat shock transcription factor family (HSFs). Traditionally, HSFs maintains protein homeostasis in cells under heat stress by regulating the expression of molecular chaperones [5, 6]. Many studies have shown that HSF1 can regulate and activate the transcription of target genes other than heat shock response-related proteins without heat stress [7-10].

In addition, HSF1 expression is increased in several cancer types including CRC [11, 12]. This may be related to the existence of various stress signals in malignant tumor cells and microenvironment, including genomic instability, abnormal cell-cell signals and oxidative stress, and these stress signals cause high expression of HSF1 [13, 14]. Several studies have shown that high expression of HSF1 plays a vital role in the survival of tumor tissues by regulating the transcription of multiple oncogenes and participating in signal crosstalk between tumor cells and extracellular stromal cells [15-20]. Regarding the role of HSF1 in CRC, several studies have revealed the molecular mechanisms by which HSF1 contributes to CRC development [18, 21, 22]. Further understanding of the molecular mechanisms through which HSF1 regulates the progression of colorectal cancer may provide clues for novel treatments that have yet to be elucidated.

Claudins are the main membrane protein that constitutes tight junctions, and its abnormal expression will not only affect intercellular adhesion, but also mediate the change of cell polarity and the transport of important molecules [23-25]. Evidence shows that the expression of multiple members of the claudins family is altered in various types of cancers and plays an important role in the occurrence, development, and metastasis of cancers [26-30]. Claudin3 (CLDN3), which belongs

to the claudins family, shows high expression in CRC tissues. The expression level of CLDN3 is closely related to the maintenance of colon epithelial barrier and the growth and invasion of CRC [31-33], indicating that CLDN3 may be a potential molecular biomarker for CRC.

In this study, we confirmed that HSF1 is associated with poor prognosis of CRC, and clarified that HSF1 can promote the proliferation, migration, and invasion of colon cancer cells. We also found that CLDN3 is a direct target gene for HSF1, which can activate the transcription of CLDN3. These results provide evidence for understanding the role and molecular regulation mechanism of HSF1 in CRC.

Materials and methods

Bioinformatics analysis. The different mRNA expression of HSF1 levels between a human patient's tumor and the adjacent normal tissues across the TCGA database was analyzed by the TIMER2.0 (http://timer.cistrome.org) online system. RNAseq-FPKM data and clinical information for CRC samples (n=698) were downloaded from UCSC Xena (http://xena.ucsc.edu/), and the relationship between HSF1 expression and clinical features was analyzed. Kaplan-Meier and Univariate and multivariate cox regression analyses were performed only on patients with complete clinical data. To find genes highly correlated to HSF1 expression levels, WGCNA analysis was performed using R package WGCNA (version 1.63) The top 10% of genes with the greatest variation in normalized count values in the TCGA colon cancer samples (n=471) were used for WGCNA. When scale-free $R^2 > 0.9$, the soft threshold is determined and other parameters are default. Then the cluster dendrogram and module are generated. The resulting modules were analyzed for correlations to HSF1 group. Hub genes were extracted by filtering on gene significance > 0.4 and module membership (MM) > 0.75. Gene Ontology (GO) and Kyoto Encyclopedia of Genes and Genomes (KEGG) enrichment analysis of HSF1-related module membership was performed using R package cluster Profiler to explore biological characteristics.

Tissue microarrays and immunohistochemistry. 111 pairs of CRC tissues and adjacent control tissues were collected from 2013-2015 surgical specimens of patients with CRC in Zhejiang Cancer Hospital, and the 111 patients were followed up. The human colon cancer tissue microarrays were prepared by KONFOONG Biotech (Ningbo, China).

TMA sections were stained using rabbit anti-HSF1 (dilution 1: 100, #51034-1-AP, Proteintech), using a standard IHC protocol. Briefly, following antigen retrieval, the sections were blocked with 0.3% solution of hydrogen peroxide (in PBS) and then incubated with primary antibody overnight at 4 °C. The detection of the antigen-antibody complex was performed using a goat anti-rabbit secondary antibody and the Streptavidin-HRP Systems kit (Dako). Images of the tissues were taken by using a light microscope (Olympus, Japan). For each sample, the H-score was calculated as staining intensity multiplied by the percentage area of positive cells, and was used as a criterion to determine the level of protein expression. The staining intensity classification is as follows: 1+ is weak staining, 2+ is moderate staining, and 3+ is strong staining.

This study was approved by the Ethical Committee of Zhejiang Cancer Hospital (IRB-2023-334). All participants were recruited after providing signed informed consent.

Cell culture. Human colon cancer cell lines RKO and HT29 and the human colon epithelial cells HCoEpiC were purchased from the Shanghai Cell Bank of the Chinese Academy of Science. The 293T cell line was purchased from the American Type Culture Collection (ATCC). All cells were cultured in DMEM medium (#C11995500BT, Gibco) supplemented with 10% fetal bovine serum (#A3160801, Gibco), 100 U/ml penicillin and 100 U/ml streptomycin (#P1400, Solarbio). All cells were incubated in a humidified environment at 37 °C with 5% CO_2, and the cell culture medium was replaced every 2 days.

Lentivirus packaging and infection. Human HSF1 overexpression lentivirus (#sc-400432-LAC) and negative control lentivirus (#sc-437282) were purchased from Santa Cruz. Human shHSF1 plasmid (SH) and negative control plasmid (NC) were purchased from GUANNAN Biotech (Hangzhou, China). The sequence of shHSF1 plasmid was CCAGCAACAGAAAGTCGTCAA. For producing lentiviruses, the pLKO.1 vector carrying HSF1 shRNA or scrambled shRNA was transfected into 293T cells with helper plasmid pVSVG, pREV and pGAG (conserved in our lab) using the Lipofectamine 3000 reagent (Invitrogen). Fresh culture medium was replaced 8 h after transfection, and the supernatant containing the virus was collected. To construct knockdown and overexpressed CRC cell lines, RKO and HT29 cells were infected with the previously obtained supernatant and HSF1 overexpressed lentivirus in the presence of polybrene for 48 h. Stably expression cells were selected with puromycin and validated by Western blotting analysis.

RNA isolation and quantitative real-time PCR (qRT-PCR). Total RNA was extracted using an RNA Fast Purification Kit (EScience, Shanghai; #RN001), and then the concentration and quality of RNA were measured. RNA reverse transcription was carried out using the Fast All-in-One RT Kit (with gDNA Remover) (EScience, Shanghai; #RT001). Reverse transcription DNA was processed with SYBR Green Master Mix (Shanghai EScience; #QP002) and detected by ABI 7500 PCR system. GAPDH was used as an internal control, and the results were calculated for relative normalized expression using the $2^{-\Delta\Delta CT}$ method. All of the PCR primers were obtained from Sangon Biotech (Shanghai, China) and the sequences of all primers are shown in Supplementary Table S1.

Western blotting. Proteins were extracted from cells using RIPA lysis buffer (78501, Thermo Fisher Scientific) containing fresh protease and phosphatase inhibitors. Cell lysates were centrifuged at 12,000 × g for 15 min at 4 °C. Protein contents in the supernatant were quantified using bicinchoninic acid (BCA) Protein Assay Kit (Pierce Thermo Scientific). Protein samples was electrophoresed on Tris-Glycine SDS Running Buffer, and then transferred onto polyvinylidene fluoride membranes (#ISEQ00010, Merck Millipore). The membranes were blocked with 5% non-fat milk (Solarbio) and maintained overnight at 4 °C with primary antibodies. After incubation with secondary antibodies (1:3,000; CST) for one hour at room temperature. The immune binding was detected using the ECL detection system (Fdbio Science Biotech). GAPDH was used as internal loading control. HSF1 polyclonal antibody (#16107-1-AP). and GAPDH polyclonal antibody were purchased from Proteintech (#10494-1-AP, Wuhan, China). Monoclonal anti-human Claudin-3 antibody was purchased from Immunoway (#YM4920, Jiangsu, China).

Colony formation assay. For colony formation, 1,000-2,000 cells were seeded in 6-well plates and cultured for 14 days with the medium changed every 3 days. At the end of the experiment, cells were fixed with 4% formaldehyde for 20 min, stained with 0.1% crystal violet solution for another 20 min. The numbers of cell colonies were counted after washing 5 times by PBS. The above assays were performed in triplicates, and the entire experiments were repeated three times.

Wound healing assay. Cell horizontal migration ability was detected by wound healing assay. The cells were cultured in 6-well plates to 80-90% confluence. A straight-line wound was made using a 10 μl pipette tip. Cell debris and smoothed the edge of the straight-line wound were removed by a wash with PBS and cells were then maintained in a medium with a reduced percentage of FBS (1%).

The wounds were photographed and measured at 0 h and 18 h using a microscope (Leica), and the wound area was quantified using ImageJ.

Cell migration and invasion assay. Vertical migration and invasion ability were detected by transwell experiment. The transwell experiment was carried out by 8 μm transwell Chambers (Corning Costar). Cells were seeded on the upper chamber of a 24-well plate at a concentration of 8 × 10^5 cells, which was coated with Matrigel (BD Biosciences). DMEM containing 1% FBS was added to the upper chamber, while the lower chamber was filled with DMEM with 20% FBS. After 24 h, the cells that migrated through the upper chamber were fixed in 4% paraformaldehyde (PFA) and stained with 0.1% crystal violet. Each chamber was washed with PBS and unmigrated cells were removed with cotton swabs. The stained cells were photographed under an inverted microscope (Leica). Five fields at 200× magnification was randomly obtained for each transwell and cell numbers were quantified using ImageJ. For transwell migration assays, transwell chambers without matrigel were used. Each condition was repeated 3 times and the data averaged.

Chromatin immunoprecipitation and ChIP-qPCR. ChIP assays were performed following the manufacturer's instructions (ChIP Assay kit, #3588650, Merck). Anti-HSF1 (#51034-1-AP, Proteintech) was used to precipitate protein-bound DNA. Anti-Mouse IgG (CST) was used as a control. Briefly, cells were crosslinked with 1% formaldehyde for 10 min at room temperature, and the reaction was stopped with 125 mM glycine. After three washes with 1× PBS, cells were lysed with SDS Lysis Buffer supplemented with protease and phosphatase inhibitors. Lysates were sonicated on ice using a Covaris M220 sonicator for 2 min (Peak incident power=75, Duty Factor=5, Cycle=100). Size of fragments obtained (between 150 bp and 800 bp) was confirmed by electrophoresis. 10 μl chromatin was taken as Input control and frozen for subsequent purification of DNA. Samples were immunoprecipitated with 2-4 μg of the appropriate antibodies overnight at 4 °C. Add Salmon Sperm DNA/Protein A Agarose Slurry and rotate at 4 °C for 1 h to collect the antibody-binding protein-DNA complex. The complexes were washed once with Low Salt Immune Complex Wash Buffer, High Salt Immune Complex Wash Buffer, LiCI Immune Complex Wash Buffer, respectively; and twice with TE Buffer. After reverse crosslinking was performed, the DNA was eluted and purified using a DNA purification kit (Beyotime). Primer1 to 3 were designed and RT-qPCR analysis was performed on three regions of the CLDN3 transcription initiation site (TSS)

from −2000 bp to + 100 bp. Primer sequences for ChIP analysis are shown in Supplementary Table S2.

Nude mice xenograft models. BALB/c nude mice (6 weeks old, female, 18.0 ± 2.0 g) were purchased from PAISIAO biotech (Hangzhou, China) and were randomly divided into indicated two groups: RKO-SH-HSF1 group, RKO-NC group. To establish the mouse xenograft model, nude mice were inoculated with 5×10^6 cells dissolved in PBS into their right armpits. After 10 days (when the tumor volume reached 120 mm^3), it was recorded as the first day and the tumor size was measured with a vernier caliper every 3 days. The formula for calculating tumor volume is as follows: TV (mm^3)=($a \times b^2$)/2, where a is the maximum diameter and b is the minimum diameter. The first day of measurement was recorded when the average tumor volume in the control group was greater than 120 mm^3. All animals were sacrificed after seven measurements, and the transplanted tumors were excised, weighed, and fixed.

All experimental procedures involving the animals were conducted in accordance with ethical standards and were approved by the Experimental Animal Ethical Committee of Zhejiang Cancer Hospital (2024-03-026).

Statistical analysis. All of the statistical analyses and visualizations were performed using R software (version 4.2.2) and GraphPad Prism 8.0 (GraphPad Software). Clinicopathological characteristics were compared between the groups using a $\chi 2$ test for dichotomous and categorical variables. Kaplan-Meier survival analysis was used for the p-values of the Log-rank tests, and the HSF1 expression with the smallest p-value was taken as the group cut-off value. Univariate and multivariate cox regression analyses were used to determine independent predictors of disease-free survival events for colon cancer. Variables with $p < 0.3$ in the univariate analysis were entered into a multivariate model. Differential expression analysis was performed using the R package edgeR (version 3.24.1). Volcano plots were generated using ggplot2 to visualize differentially expressed genes. Log-fold change $\geq$ 0.58 and $p < 0.05$ were deemed the threshold for selecting differentially expressed genes (DEGs) [34, 35]. Pearson correlation coefficient was used to evaluate the correlation between HSF1 and CLDN3, as well as YIF1A expressions, which was presented by scatter plot. All results were expressed as mean±SEM, and statistical significance was assessed using Mann-Whitney test or the one sample t-test when appropriate at the significance level (p)

indicated. Significance for all statistical tests was shown in figures for not significant (NS), *p < 0.05, **p < 0.01, ***p < 0.001 and ****p < 0.0001.

Results

High expression of HSF1 is associated with worse outcome in CRC. To understand the expression of HSF1 in several types of cancers, we used the Gene_DE module of the Timer2 (http://timer.cistrome.org) platform to analyze the differential expression of HSF1 in tumor and adjacent normal tissues from the Cancer Genome Atlas (TCGA). The results showed that HSF1 expression levels were significantly higher in tumor tissues than in adjacent normal tissues, including colon cancer and rectal cancer cohorts (Figure 1A). As for the clinical significance of HSF1, we first analyzed the relationship between HSF1 expression and clinicopathological parameters based on the CRC cohort (COADREAD) in TCGA. We found that the expression of HSF1 was higher in the subgroups with higher pathological stage, N stage, M stage, and lymphatic invasion (Figure 1B). The expression of HSF1 no significant difference in between T stage subgroups (Figure 1B). According to Kaplan-Meier analysis, then we found that high HSF1 expression was associated with shorter overall survival (p=0.036), disease-specific survival (p=0.005) and disease-free survival (p=0.022). In conclusion, these research results suggest that the overexpression level of HSF1 is associated with the adverse clinical features and worse survival prognosis of CRC.

To verify these findings, we collected 111 cases of colon cancer patients' tumor and adjacent tissues from the hospital, and then constructed tissue microarrays (s). We summarized the clinical and pathological features based on the tumor HSF1 expression level in Table 1. Immunohistochemical staining showed that HSF1 was moderately to strongly expressed in colorectal cancer cells, mainly located in the nucleus and a small amount in the cytoplasm, suggesting that HSF1 may play an important role in transcriptional regulation in these regions (Figure 2A). Quantitative analysis showed that HSF1 expression levels were significantly higher in tumor tissues than in adjacent normal tissues (Figure 2B). Kaplan-Meier analysis and Cox regression analysis were used to evaluate the prognostic significance of HSF1 expression in patients with CRC. The Kaplan-Meier analysis demonstrated that high HSF1 expression was associated with shorter disease-free survival

(p=0.013; Figure 2C). Univariate and multivariate analyses indicated that HSF1 expression and M staging could be used as independent prognostic indicators for disease-free survival events in patients with CRC (Figure 2D). In summary, high expression of HSF1 in 111 patients with CRC is associated with poor prognosis and may serve as a promising prognostic biomarker.

HSF1 promotes the proliferation, migration and invasion of CRC. As CRC is a highly heterogeneous disease, we quantified the level of HSF1 protein in various CRC cell lines. Compared to normal human colon epithelial cell lines, human colon cancer cell lines exhibit high HSF1 expression (Figure 3A). To evaluate the cellular function of HSF1, we constructed stable HSF1 knockdown and overexpression in RKO and HT29 (Figure 3B). The plate colony formation assay showed that, compared with the control group, HSF1 overexpression promoted the clonogenic potential of CRC cells, while HSF1 knockdown reduced the clonogenic potential of CRC cells (Figure 3C). Due to the distinct growth characteristics of CRC cell lines, we evaluated the migration and invasion of colon cancer cells through scratch healing, transwell migration, and matrigel invasion assays. The wound healing experimental results in RKO lines showed that overexpression of HSF1 significantly increased the wound closure area at 18h after scratching, while inhibition of HSF1 decreased the wound closure area (Figure 3D). Similarly, in transwell migration and invasion assays in RKO and HT-29 lines, knockdown of HSF1 significantly inhibited colon cells migration and invasion (Figure 3E). Overall, we demonstrated that the expression of HSF1 can affect clonogenic potential, migration, and invasion of CRC cells.

HSF1 promotes growth of CRC cells *in vivo*. To further investigate if HSF1 is required for tumor growth *in vivo*, we assessed the impact of HSF1 knockout on the *in vivo* tumorigenicity of the RKO cells subcutaneously xenografted into nude mice (Figure 4A). Data showed that the transplanted tumors grew slowly and volume and weight of the transplanted tumors were significantly decreased in the SH-HSF1 group compared with the control group (Figures 4B, 4C). There was no statistically significant difference in total body weight, between the two groups of mice at all time points (Figure 4D). Together, these results suggested that HSF1 plays an important role in tumor formation in mice.

The association between HSF1 expression and CLDN3 expression in CRC. To further explore the downstream molecules regulated by HSF1 in colon cancer, we identified genes associated with

HSF1 expression using weighted gene co-expression network analysis (WGCNA) and data from 471 samples of colon cancer from TCGA [36]. WGCNA identified six co-expression modules that were differentially expressed between the low and high HSF1 expression groups (Figure 5A). The correlation analysis between the six modules and phenotypes showed that the turquoise module had a strong correlation between the low and high HSF1 expression in colon cancer (Figures 5B, 5C). Combined with differential analysis, the 10 most differentially expressed hubgenes in the turquoise module were screened, of which CLDN3 exhibited the greatest fold difference (Figure 5D). Next, we examined the expression levels of the 10 most differentially expressed genes in stable RKO cell lines with HSF1 knockdown. As expected, we demonstrated that HSF1 knockdown significantly decreased the mRNA levels of CLDN3 and increased levels of Yip1 Interacting Factor Homolog A (YIF1A) (Figure 5E). The scatter plot showed that HSF1 expression was significantly positively correlated with the expression of CLDN3 and YIF1A in CRC. However, previous experimental validation results indicated that the mRNA expression level of YIF1A was negatively correlated with HSF1. Due to the inconsistency in the conclusions regarding YIF1A expression, we decided not to proceed with further research on YIF1A in this study (Figure 5F). To further determine the protein expression level of CLDN3 in cell lines, western blot results confirmed that claudin-3 expression was positively correlated with HSF1 (Figure 5G). Thus, we reasonable speculated that HSF1 may promote the expression of CLDN3 in colon cancer at the transcriptional level without exogeneous stress.

In order to further understand the function of genes related to CLDN3 and HSF1, the GO and KEGG pathway analysis of the turquoise module and CLDN3 related items were listed separately. The results showed that the functions and pathways of CLDN3 are enriched in regulation of cell biogenesis, response to oxygen levels, and composition of cell-cell connection functional annotations and pathways (Figure 5G). To a certain extent, WGCNA analysis provides biological insights into the ways in which HSF1 co-expressed genes are involved in promoting cancer.

CLDN3 is a novel HSF1 target gene in CRC. We reasonably hypothesized that HSF1 might bind to the promoter region of the CLDN3 gene as a transcription factor, thereby regulating the expression of claudin3 at the transcriptional level. We analyzed and predicted transcription factor binding elements of HSF1 using the JASPAR database (https://jaspar.genereg.net) (Figure 6A), and

identified a potential HSF1 binding site in the gene promoters of CLDN3 (Figure 6B). It has been shown that transcription factor binding sites (TFBS) are usually located 2 kb upstream of the transcription start site (TSS) [37]. Moreover, we designed three primer pairs covering the −2000 to +100 bp region relative to the transcription start site (TSS) of CLDN3 (Figure 6C), and examined chromatin immunoprecipitation (ChIP) assays to quantify HSF1 occupancy in the relative regions of the three primer pairs. As shown in Figure 6D, HSF1 antibody immunoprecipitated the sequences amplified by Primer 1, demonstrating direct interactions of HSF1 with promoters of CLDN3 in the parental RKO cells. The relative enrichment of HSF1 was assessed by quantitative polymerase chain reaction (qPCR), which revealed nearly threefold higher levels of HSF1 occupancy in regions amplified by primer 1, compared with immunoprecipitations with control IgG (Figure 6E). Accordingly, HSF1 directly activates CLDN3 transcription in colon cancer, possibly supporting colon cancer progression through this pathway.

Discussion

As an evolutionarily conserved transcription factor, HSF1 can respond to intracellular and extracellular stresses, target the promoters of heat shock proteins, activate the expression of heat shock proteins, and thereby play a role in maintaining intracellular protein homeostasis [5, 38]. Under the context of cancer, HSF1 can be activated by various stimuli in addition to traditional heat stress. Activated HSF1 can target many cancer-specific genes, and oncogenes regulated by HSF1 jointly support the survival of tumor cells [6, 13, 14]. Multiple evidences indicate that the target genes regulated by HSF1 can act on tumor cells, stromal cells or immune cells in the microenvironment, such as directly affecting the proliferation, apoptosis, and metabolic reprogramming of cancer cells, mediating the regulation of fibroblasts on the extracellular matrix, and mediating the release of cytokines that recruit immune cells [16, 39-43].

According to reports on the clinical significance of HSF1, it has been basically confirmed that HSF1 is associated with poor prognosis and adverse clinical events in various cancers, including CRC [11, 44]. Moreover, the efficacy of HSF1 as a new therapeutic target in combination with other therapies has been preliminarily validated [45-49]. This indicates that HSF1 might be useful as potential prognostic factors and therapeutic targets, but further studies will be required to better

understand of its carcinogenic molecular mechanisms.

We examined HSF1 levels in TCGA database and tissues of 111 patients with CRC, and explored its clinical significance in CRC. Our research results confirmed that the mRNA and protein levels of HSF1 were significantly upregulated in CRC compared with normal tissues, and high expression of HSF1 was an independent poor prognostic factor. Analysis of clinical features found that HSF1 expression level was obviously associated with N stage, M stage and lymphatic metastasis. Interestingly, through analyzing the clinical features of 111 patients, it was found that the expression level of HSF1 was associated with microsatellite status, and microsatellite instability typically predicts better immunotherapy efficacy [50], suggesting that HSF1 expression levels might be linked to immunotherapy outcomes.

To discuss the role of HSF1 in CRC and its new regulatory mechanism, we conducted bioinformatics analysis and functional validation *in vitro* and *in vivo*. Consistent with previous reports, HSF1 could positively regulate the clonogenic potential, invasion, and migration of RKO and HT29 cells, and promote the growth of transplanted tumors in mice. Then, we analyzed the gene modules associated with higher HSF1 expression using WGCNA based on TCGA. In the verification of mRNA expression levels of the 10 most differentially expressed hubgenes in the turquoise module, we found that CLDN3 and HSF1 expressions showed a positive correlation, which was consistent with the analysis results, indicating that HSF1 might positively regulate CLDN3. There is currently no direct evidence that HSF 1 regulates the expression of CLDN 3 in colon cancer, and this possibility warrants further investigation. Therefore, we demonstrated that CLDN3 is the direct target gene of HSF1 by ChIP-seq assay, and HSF1 can induce gene transcription of CLDN3. In the GO and KEGG functional clustering of the turquoise module, the function of HSF1-mediated CLDN3 is mainly related to the formation of tight junction structure, molecular transport of cell membrane, and response to oxygen levels.

CLDN3 is the encoding gene of claudin3, which belongs to the claudins protein family that is under hot research. Zolbetuximab, a drug targeting Claudin-18.2, has demonstrated effectiveness in Phase I clinical trials for gastric cancer [51], while other basic research and drug development centered around claudins are also underway. Many studies have demonstrated that claudin 3 is involved in tight junction barrier function, which can regulate the permeability of ions, solutes and proteins to

cells by regulating their distribution in tight junctions to maintain barrier integrity [52-54]. There are some pharmacological studies on claudin3 molecular transport function, such as CLDN3 regulates cisplatin sensitivity by controlling the expression of cisplatin influx transporter CTR1 [55], but there are few relevant basic studies in tumor cells. CLDN3 is currently used as a cancer biomarker to induce the malignant potential of CRC [32, 33, 56], for example, overexpressed CLDN3 promotes cell migration of CRC cell line HT29 cells and increases malignant transformation [31]. Therefore, our results identified that HSF1 directly binds to the promoter region of CLDN3 and activates the transcription of CLDN3, while the specific molecular mechanism requires further investigation, which may have prognostic value and provide targets for therapeutic intervention in the future.

In conclusion, we demonstrated that HSF1 has a carcinogenic effect on CRC and is associated with adverse clinical outcomes. HSF1 upregulates the expression of claudin3 by binding to the CLDN3 promoter region, which may affect the malignant potential of colon cancer cells. Our data suggest that the novel mechanism may have considerable potential as a prognostic predictor and therapeutic target in CRC.

Acknowledgements: This work was supported by grants Department of Science and Technology of State Administration of Traditional Chinese Medicine-Zhejiang Provincial Administration of Traditional Chinese Medicine Joint Science and Technology Project (GZY-ZJ-KJ-24005), Zhejiang Provincial Traditional Chinese Medicine Health Project (2022ZA030), Zhejiang Provincial Medicine and Health Technology Project (2024KY797), The Science and Technology Plan Project of Zhejiang Province (2021C03106).

Supplementary data are available in the online version of the paper.

References

[1] DEKKER E, TANIS PJ, VLEUGELS JLA, KASI PM, WALLACE MB. Colorectal cancer. Lancet 2019; 394: 1467-1480. https://doi.org/10.1016/S0140-6736(19)32319-0

[2] SUNG H, FERLAY J, SIEGEL RL, LAVERSANNE M, SOERJOMATARAM I et al. Global Cancer Statistics 2020: GLOBOCAN Estimates of Incidence and Mortality Worldwide for

36 Cancers in 185 Countries. CA Cancer J Clin 2021; 71: 209-249. https://doi.org/10.3322/caac.21660

[3] BOEHM JE, ROHAN EA, PREISSLE J, DEGROFF A, GLOVER-KUDON R. Recruiting patients into the CDC's Colorectal Cancer Screening Demonstration Program: strategies and challenges across 5 sites. Cancer 2013; 15: 2914-2925. https://doi.org/10.1002/cncr.28161

[4] MILLER KD, NOGUEIRA L, MARIOTTO AB, ROWLAND JH, YABROFF KR et al. Cancer treatment and survivorship statistics, 2019. CA Cancer J Clin 2019; 69: 363-385. https://doi.org/10.3322/caac.21565

[5] AKERFELT M, MORIMOTO RI, SISTONEN L. Heat shock factors: integrators of cell stress, development and lifespan. Nat Rev Mol Cell Biol 2010; 11: 545-555. https://doi.org/10.1038/nrm2938

[6] GOMEZ-PASTOR R, BURCHFIEL ET, THIELE DJ. Regulation of heat shock transcription factors and their roles in physiology and disease. Nat Rev Mol Cell Biol 2018; 19: 4-19. https://doi.org/10.1038/nrm.2017.73

[7] DAI C. The heat-shock, or HSF1-mediated proteotoxic stress, response in cancer: from proteomic stability to oncogenesis. Philos Trans R Soc Lond B Biol Sci 2018; 373: 20160525. https://doi.org/10.1098/rstb.2016.0525

[8] ZHOU Z, LI Y, JIA Q, WANG Z, WANG X et al. Heat shock transcription factor 1 promotes the proliferation, migration and invasion of osteosarcoma cells. Cell Prolif 2017; 50: e12346. https://doi.org/10.1111/cpr.12346

[9] SURAL S, LIANG CY, WANG FY, CHING TT, HSU AL. HSB-1/HSF-1 pathway modulates histone H4 in mitochondria to control mtDNA transcription and longevity. Sci Adv 2020; 6: eaaz4452. https://doi.org/10.1126/sciadv.aaz4452

[10] TANG Z, DAI S, HE Y, DOTY RA, SHULTZ LD et al. MEK guards proteome stability and inhibits tumor-suppressive amyloidogenesis via HSF1. Cell 2015; 160: 729-744. https://doi.org/10.1016/j.cell.2015.01.028

[11] CHEN F, FAN Y, CAO P, LIU B, HOU J et al. Pan-Cancer Analysis of the Prognostic and Immunological Role of HSF1: A Potential Target for Survival and Immunotherapy. Oxid Med Cell Longev 2021; 2021: 5551036. https://doi.org/10.1155/2021/5551036

[12] WANG H, WANG X, ZHANG H, DENG T, LIU R et al. The HSF1/miR-135b-5p axis induces protective autophagy to promote oxaliplatin resistance through the MUL1/ULK1 pathway in colorectal cancer. Oncogene 2021; 40: 4695-4708. https://doi.org/10.1038/s41388-021-01898-z

[13] SCHERZ-SHOUVAL R, SANTAGATA S, MENDILLO ML, SHOLL LM, BEN-AHARON I et al. The reprogramming of tumor stroma by HSF1 is a potent enabler of malignancy. Cell 2014; 158: 564-578. https://doi.org/10.1016/j.cell.2014.05.045

[14] ALTORKI NK, MARKOWITZ GJ, GAO D, PORT JL, SAXENA A et al. The lung microenvironment: an important regulator of tumour growth and metastasis. Nat Rev Cancer 2019; 19: 9-31. https://doi.org/10.1038/s41568-018-0081-9

[15] FERRARI N, RANFTL R, CHICHEROVA I, SLAVEN ND, MOEENDARBARY E et al. Dickkopf-3 links HSF1 and YAP/TAZ signalling to control aggressive behaviours in cancer-associated fibroblasts. Nat Commun 2019; 10: 130. https://doi.org/10.1038/s41467-018-07987-0

[16] JACOBS C, SHAH S, LU WC, RAY H, WANG J et al. HSF1 inhibits antitumor immune activity in breast cancer by suppressing CCL5 to block CD8+ T cell recruitment. Cancer Res 2024; 84: 276-290. https://doi.org/10.1158/0008-5472.CAN-23-0902

[17] GRUNBERG N, PEVSNER-FISCHER M, GOSHEN-LAGO T, DIMENT J, STEIN Y et al. Cancer-Associated Fibroblasts Promote Aggressive Gastric Cancer Phenotypes via Heat Shock Factor 1-Mediated Secretion of Extracellular Vesicles. Cancer Res 2021; 81: 1639-1653. https://doi.org/10.1158/0008-5472.CAN-20-2756

[18] LI J, SONG P, JIANG T, DAI D, WANG H et al. Heat Shock Factor 1 Epigenetically Stimulates Glutaminase-1-Dependent mTOR Activation to Promote Colorectal Carcinogenesis. Mol Ther 2018; 26: 1828-1839. https://doi.org/10.1016/j.ymthe.2018.04.014

[19] YANG W, FENG B, MENG Y, WANG J, GENG B et al. FAM3C-YY1 axis is essential for TGFβ-promoted proliferation and migration of human breast cancer MDA-MB-231 cells via the activation of HSF1. J Cell Mol Med 2019; 23: 3464-3475. https://doi.org/10.1111/jcmm.14243

[20] WANG B, LEE CW, WITT A, THAKKAR A, INCE TA. Heat shock factor 1 induces cancer stem cell phenotype in breast cancer cell lines. Breast Cancer Res Treat 2015; 153: 57-66. https://doi.org/10.1007/s10549-015-3521-1

[21] SONG P, FENG L, LI J, DAI D, ZHU L. β-catenin represses miR455-3p to stimulate m6A modification of HSF1 mRNA and promote its translation in colorectal cancer. Mol Cancer 2020; 19: 129. https://doi.org/10.1186/s12943-020-01244-z

[22] XU SM, LIU XZ, WANG L, HUANG WH, HU YT et al. Synergistic anticancer activity of HSP70 and HSF1 inhibitors in colorectal cancer cells: A new strategy for combination therapy. Biochim Biophys Acta Mol Basis Dis 2024; 1871: 167630. https://doi.org/10.1016/j.bbadis.2024.167630

[23] HAGEN SJ. Non-canonical functions of claudin proteins: Beyond the regulation of cell-cell adhesions. Tissue Barriers 2017; 5: e1327839. https://doi.org/10.1080/21688370.2017.1327839

[24] KIM JJ, KIM N, PARK JH, KIM YS, LEE SM et al. Comparison of Tight Junction Protein-Related Gene mRNA Expression Levels between Male and Female Gastroesophageal Reflux Disease Patients. Gut Liver 2018; 12: 411-419. https://doi.org/10.5009/gnl17419

[25] LI JN, ZHANG Z, WU GZ, YAO DB, CUI SS. Claudin-15 overexpression inhibits proliferation and promotes apoptosis of Schwann cells in vitro. Neural Regen Res 2020; 15: 169-177. https://doi.org/10.4103/1673-5374.264463

[26] LU S, SINGH K, MANGRAY S, TAVARES R, NOBLE L et al. Claudin expression in high-grade invasive ductal carcinoma of the breast: correlation with the molecular subtype. Mod Pathol 2013; 26: 485-495. https://doi.org/10.1038/modpathol.2012.187

[27] LUO J, CHIMGE NO, ZHOU B, FLODBY P, CASTALDI A et al. CLDN18.1 attenuates malignancy and related signaling pathways of lung adenocarcinoma in vivo and in vitro. Int J Cancer 2018; 143: 3169-3180. https://doi.org/10.1002/ijc.31734

[28] ZHOU Y, XIANG J, BHANDARI A, GUAN Y, XIA E et al. CLDN10 is Associated with Papillary Thyroid Cancer Progression. J Cancer 2018; 9: 4712-4717. https://doi.org/10.7150/jca.28636

[29] SINGH AB, SHARMA A, SMITH JJ, KRISHNAN M, CHEN X et al. Claudin-1 up-regulates the repressor ZEB-1 to inhibit E-cadherin expression in colon cancer cells. Gastroenterology 2011; 141: 2140-2153. https://doi.org/10.1053/j.gastro.2011.08.038

[30] YUAN M, CHEN X, SUN Y, JIANG L, XIA Z et al. ZDHHC12-mediated claudin-3 S-palmitoylation determines ovarian cancer progression. Acta Pharm Sin B 2020; 10: 1426-1439. https://doi.org/10.1016/j.apsb.2020.03.008

[31] DE SOUZA WF, FORTUNATO-MIRANDA N, ROBBS BK, DE ARAUJO WM, DE-FREITAS-JUNIOR JC et al. Claudin-3 overexpression increases the malignant potential of colorectal cancer cells: roles of ERK1/2 and PI3K-Akt as modulators of EGFR signaling. PLoS One 2013; 8: e74994. https://doi.org/10.1371/journal.pone.0074994

[32] PÉREZ AG, ANDRADE-DA-COSTA J, DE SOUZA WF, DE SOUZA FERREIRA M, BORONI M et al. N- glycosylation and receptor tyrosine kinase signaling affect claudin- 3 levels in colorectal cancer cells. Oncol Rep 2020; 44: 1649-1661. https://doi.org/10.3892/or.2020.7727

[33] WANG Y, SUN T, SUN H, YANG S, LI D et al. SCF/C-Kit/JNK/AP-1 Signaling Pathway Promotes Claudin-3 Expression in Colonic Epithelium and Colorectal Carcinoma. Int J Mol Sci 2017; 18: 765. https://doi.org/10.3390/ijms18040765

[34] LOVE MI, HUBER W, ANDERS S. Moderated estimation of fold change and dispersion for RNA-seq data with DESeq2. Genome biol 2014; 15: 550. https://doi.org/10.1186/s13059-014-0550-8

[35] ROBINSON MD, MCCARTHY DJ, SMYTH GK. edgeR: a Bioconductor package for differential expression analysis of digital gene expression data. Bioinformatics 2010; 26: 139-140. https://doi.org/10.1093/bioinformatics/btp616

[36] LANGFELDER P, HORVATH S. WGCNA: an R package for weighted correlation network analysis. BMC Bioinformatics 2008; 9: 559. https://doi.org/10.1186/1471-2105-9-559

[37] BOYER LA, LEE TI, COLE MF, JOHNSTONE SE, LEVINE SS et al. Core transcriptional regulatory circuitry in human embryonic stem cells. Cell 2005; 122: 947-956. https://doi.org/10.1016/j.cell.2005.08.020

[38] HOME T, JENSEN RA, RAO R. Heat shock factor 1 in protein homeostasis and oncogenic signal integration. Cancer Res 2015; 75: 907-912. https://doi.org/10.1158/0008-5472.CAN-14-2905

[39] DAI S, TANG Z, CAO J, ZHOU W, LI H et al. Suppression of the HSF1-mediated proteotoxic stress response by the metabolic stress sensor AMPK. EMBO J 2015; 34: 275-293. https://doi.org/10.15252/embj.201489062

[40] VYDRA N, JANUS P, TOMA-JONIK A, STOKOWY T, MROWIEC K et al. 17 β-Estradiol Activates HSF1 via MAPK Signaling in ER α-Positive Breast Cancer Cells. Cancers 2019; 11. https://doi.org/10.3390/cancers11101533

[41] GAGLIA G, RASHID R, YAPP C, JOSHI GN, LI CG et al. HSF1 phase transition mediates stress adaptation and cell fate decisions. Nat Cell Biol 2020; 22: 151-158. https://doi.org/10.1038/s41556-019-0458-3

[42] FERNANDO TM, MARULLO R, PERA GRESELY B, PHILLIP JM, YANG SN et al. BCL6 Evolved to Enable Stress Tolerance in Vertebrates and Is Broadly Required by Cancer Cells to Adapt to Stress. Cancer Discov 2019; 9: 662-679. https://doi.org/10.1158/2159-8290.CD-17-1444

[43] TYAGI K, MANDAL S, ROY A. Recent advancements in therapeutic targeting of the Warburg effect in refractory ovarian cancer: A promise towards disease remission. Biochim Biophys Acta Rev Cancer 2021; 1876: 188563. https://doi.org/10.1016/j.bbcan.2021.188563
[44] REN X, ZHANG L, MA X, LI J, LU Z. Integrated bioinformatics and experiments reveal the roles and driving forces for HSF1 in colorectal cancer. Bioengineered 2022; 13: 2536-2552. https://doi.org/10.1080/21655979.2021.2018235
[45] KANG H, OH T, BAHK YY, KIM GH, KAN SY et al. HSF1 Regulates Mevalonate and Cholesterol Biosynthesis Pathways. Cancers (Basel) 2019; 11: 1363. https://doi.org/10.3390/cancers11091363
[46] SHEN JH, CHEN PH, LIU HD, HUANG DA, LI MM et al. HSF1/AMPKα2 mediated alteration of metabolic phenotypes confers increased oxaliplatin resistance in HCC cells. Am J Cancer Res 2019; 9: 2349-2363.
[47] VYDRA N, JANUS P, KUS P, STOKOWY T, MROWIEC K et al. Heat shock factor 1 (HSF1) cooperates with estrogen receptor α (ERα) in the regulation of estrogen action in breast cancer cells. Elife 2021; 10: e69843. https://doi.org/10.7554/eLife.69843
[48] FOK JHL, HEDAYAT S, ZHANG L, ARONSON LI, MIRABELLA F et al. HSF1 Is Essential for Myeloma Cell Survival and A Promising Therapeutic Target. Clin Cancer Res 2018; 24: 2395-2407. https://doi.org/10.1158/1078-0432.CCR-17-1594
[49] LEVI-GALIBOV O, LAVON H, WASSERMANN-DOZORETS R, PEVSNER-FISCHER M, MAYER S et al. Heat Shock Factor 1-dependent extracellular matrix remodeling mediates the transition from chronic intestinal inflammation to colon cancer. Nat Commun 2020; 11: 6245. https://doi.org/10.1038/s41467-020-20054-x
[50] KIM TM, LAIRD PW, PARK PJ. The landscape of microsatellite instability in colorectal and endometrial cancer genomes. Cell 2013; 155: 858-868. https://doi.org/10.1016/j.cell.2013.10.015
[51] QI C, GONG J, LI J, LIU D, QIN Y et al. Claudin18.2-specific CAR T cells in gastrointestinal cancers: phase 1 trial interim results. Nat Med 2022; 28: 1189-1198. https://doi.org/10.1038/s41591-022-01800-8
[52] JANG H, LEE J, PARK S, KIM JS, SHIM S et al. Baicalein Mitigates Radiation-Induced Enteritis by Improving Endothelial Dysfunction. Front Pharmacol 2019; 10: 892. https://doi.org/10.3389/fphar.2019.00892
[53] ZAYTSOFF SJM, LYONS SM, GARNER AM, UWIERA RRE, ZANDBERG WF et al. Host responses to Clostridium perfringens challenge in a chicken model of chronic stress. Gut Pathog 2020; 12: 24. https://doi.org/10.1186/s13099-020-00362-9
[54] RAYA-SANDINO A, LOZADA-SOTO KM, RAJAGOPAL N, GARCIA-HERNANDEZ V, LUISSINT AC et al. Claudin-23 reshapes epithelial tight junction architecture to regulate barrier function. Nat Commun 2023; 14: 6214. https://doi.org/10.1038/s41467-023-41999-9
[55] SHANG X, LIN X, MANOREK G, HOWELL SB. Claudin-3 and claudin-4 regulate sensitivity to cisplatin by controlling expression of the copper and cisplatin influx transporter CTR1. Mol Pharmacol 2013; 83: 85-94. https://doi.org/10.1124/mol.112.079798
[56] LIU W, KUAI Y, WANG D, CHEN J, XIONG F et al. PPM1G Inhibits Epithelial-Mesenchymal Transition in Cholangiocarcinoma by Catalyzing TET1 Dephosphorylation for Destabilization to Impair Its Targeted Demethylation of the CLDN3 Promoter. Adv Sci (Weinh) 2024; 11: e2407323. https://doi.org/10.1002/advs.202407323

569

570 **Figure Legends**

571

572 **Figure 1.** HSF1 expression is upregulated and associated with adverse clinical events in CRC. A)
573 The mRNA level of HSF1 in tumors and their respective normal tissues from TCGA patients with
574 the indicated cancer types. TPM, transcripts per kilobase of exon model per million mapped reads.
575 B) Analysis of HSF1 expression in different clinical subgroups from CRC patients, including
576 pathological stage, TNM stage, lymphatic invasion. FPKM, fragments per kilobase of transcript per
577 million mapped reads. C) Kaplan-Meier curves of overall survival, disease specific survival and
578 disease-free survival based on TCGA-COADREAD (information complete only), comparing
579 survival between high and low expression of HSF1 (grouped according to minimum p-value). The
580 statistical significance computed by the Wilcoxon test is annotated by the number of stars (*$p <$
581 0.05; **$p < 0.01$; ***$p < 0.001$).

582

583 **Figure 2.** HSF1 was upregulated in human colon cancer tissues and associated with poor prognosis.
584 A) Representative images of HSF1 immunohistochemical staining in colon tumor tissues and
585 matched adjacent tissues of a tissue microarray (TMA). B) Quantitative analysis of relative protein
586 expression level of HSF1 in colon tumor tissues (n=111) and adjacent tissues (n=111). Data
587 represent mean±SEM (***$p < 0.001$). C) Kaplan-Meier curves of disease-free survival in patients
588 (n=111) with colon cancer, comparing survival between high and low relative protein expression
589 level of HSF1 (grouped according to minimum p-value). D) Univariate Cox regression analysis and
590 Multivariate Cox regression analysis of clinicopathological features and the expression of HSF1.

591

592 **Figure 3.** The effects of HSF1 on colony formation, migration and invasion of colon cancer cells. A)
593 HSF1 protein expression in normal intestinal epithelium and colon cancer cell lines. B) Verification
594 of HSF1 stable overexpression (OE) and knockdown cell lines (SH). C) Colony formation assays in
595 RKO and HT29 cell lines with HSF1 knockdown or overexpression. D) Wound healing assays in
596 RKO cell lines with HSF1 knockdown or overexpression. E) Transwell migration and invasion
597 assays in RKO and HT29 cell lines with HSF1 knockdown. All statistical data are expressed as

means±SEM (Student's t test, *p < 0.05; **p <0.01; ***p <0.001).

Figure 4. HSF1 promotes growth of colon cancer cells *in vivo*. A) The xenograft experiments in nude mice. B) Subcutaneous tumor weights of xenografts from RKO cells with or without knockdown HSF1 expression. C, D) Tumor growth and mouse body weights of xenografts from RKO cells with or without knockdown HSF1 expression at all-time points.

Figure 5. The association between HSF1 expression and CLDN3 expression in CRC. A) Topological overlap matrix (TOM) plot. The colors of the axes represent respective modules. The intensity of the yellow inside the heatmap represents the overlap degree of overlap, with a darker yellow representing an increased overlap. B) Heat map of the correlation between module eigengenes and HSF1 expression. Each cell contains the correlation coefficients which correspond to the cell color; blue represents negative correlation and red represents positive correlation. The P-values are stated in the brackets. C) Scatter plot of High HSF1 expression vs MM in the turquoise module. D) Volcano plot represents the differential genes between low HSF1 and high HSF1 samples from TCGA-COAD, marking the 10 most differentially expressed genes in the turquoise module. E) The mRNA expression of 10 most differentially expressed hubgenes in RKO cell lines was detected by qRT-PCR. F) Scatter plot showing the relationship between HSF1 and the expression of CLDN3 and YIF1A in CRC, respectively. G) The expression level of claudin-3 in HSF1 knockdown cell lines was detected by western blotting. H) Gene Ontology (GO) terms and Kyoto Encyclopedia of Genes and Genomes (KEGG) pathways enrichment analysis of turquoise module genes, presenting CLDN3-related terms. (*p < 0.05; **p <0.01; ***p <0.001)

Figure 6. HSF1 binds to the CLDN3 promoter to initiate CLDN3 expression in CRC. A) The transcription factor binding elements of HSF1 predicted by JASPAR. B) JASPAR predicts possible transcription factor binding sites of HSF1 on CLDN3. Start and end are counted from the first base of the input. C) Schematic of the CLDN3 gene, indicating positions of primer pairs used in ChIP-qPCR analysis. Label the opposite strand of the prediction sequence D, E) ChIP-qPCR assay of RKO-NC and RKO-SH cell lines following immunoprecipitation with anti-HSF1 antibody and

627 immunoglobulin G (IgG). %Input=Input DNA / ChIP target DNA × 100%. Fold Enrichment=ChIP
628 target DNA / Negative Control DNA. Data represent the mean±SEM (*p < 0.05; **p < 0.01; ***p <
629 0.001, multiple unpaired t-test)

630 **Table 1.** The relationship between HSF1 protein levels and clinicopathologic characteristic of
631 patients with colon cancer.

Characteristics	Low (n=56)	High (n=55)	$\chi 2$	p-value
sex, n (%)			0.009	0.926
Female	27 (24.3%)	27 (24.3%)		
Male	29 (26.1%)	28 (25.2%)		
age, n (%)			1.517	0.218
≥ 60	32 (28.8%)	25 (22.5%)		
< 60	24 (21.6%)	30 (27.0%)		
Tumor location, n (%)			1.591	0.451
Ascending Colon	33 (30%)	29 (26.4%)		
Descending Colon	7 (6.4%)	5 (4.5%)		
Transverse Colon	15 (13.6%)	21 (19.1%)		
Histological grade, n (%)			5.476	0.104
G1+G2	39 (36.1%)	44 (40.8%)		
G3	16 (14.9%)	9 (8.4%)		
T stage, n (%)			3.072	0.215
T4	38 (34.2%)	34 (30.6%)		
T3	14 (12.6%)	20 (18.0%)		
T2	4 (3.6%)	1 (0.9%)		
N stage, n (%)			0.049	0.975
N0	31 (27.9%)	31 (27.9%)		
N1+N2	25 (22.5%)	24 (21.6%)		
M stage, n (%)			0.000	1.000
M0	51 (45.9%)	51 (45.9%)		
M1	5 (4.5%)	4 (3.6%)		
AJCC stage, n (%)			1.289	0.732
I-II	29 (26.1%)	30 (27.0%)		
III-IV	27 (24.3%)	25 (22.5%)		
MMR, n (%)			0.702	0.402
pMMR	42 (40.0%)	46 (43.8%)		
dMMR	10 (9.5%)	7 (6.7%)		
Microsatellite status, n (%)			4.247	0.039*
MSI	25 (23.8%)	36 (34.3%)		
MSS	17 (16.2%)	27 (25.7%)		

632 Note: *statistically significant $p < 0.05$

Fig. 1 [Download full resolution image]

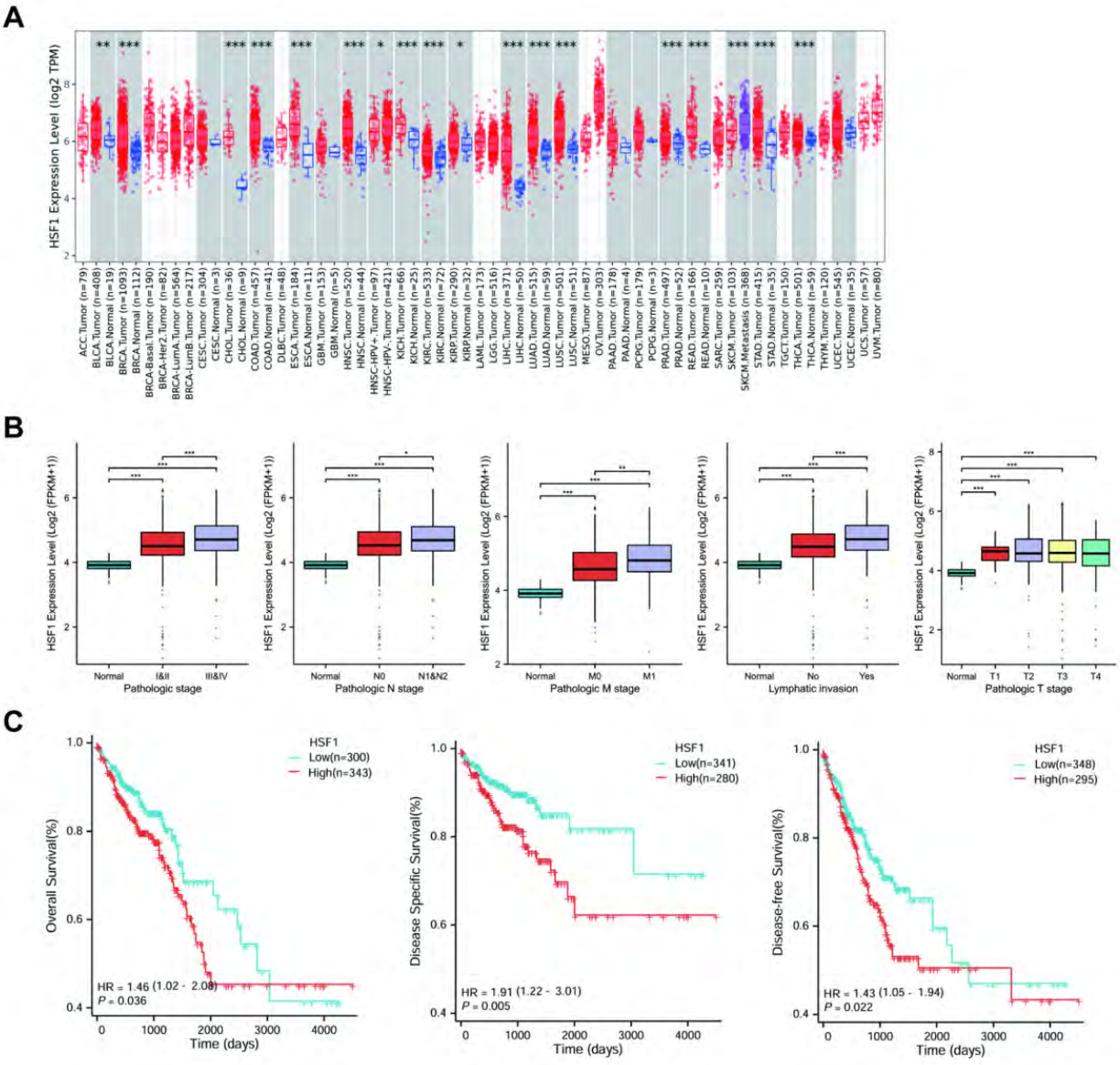

Fig. 2 [Download full resolution image]

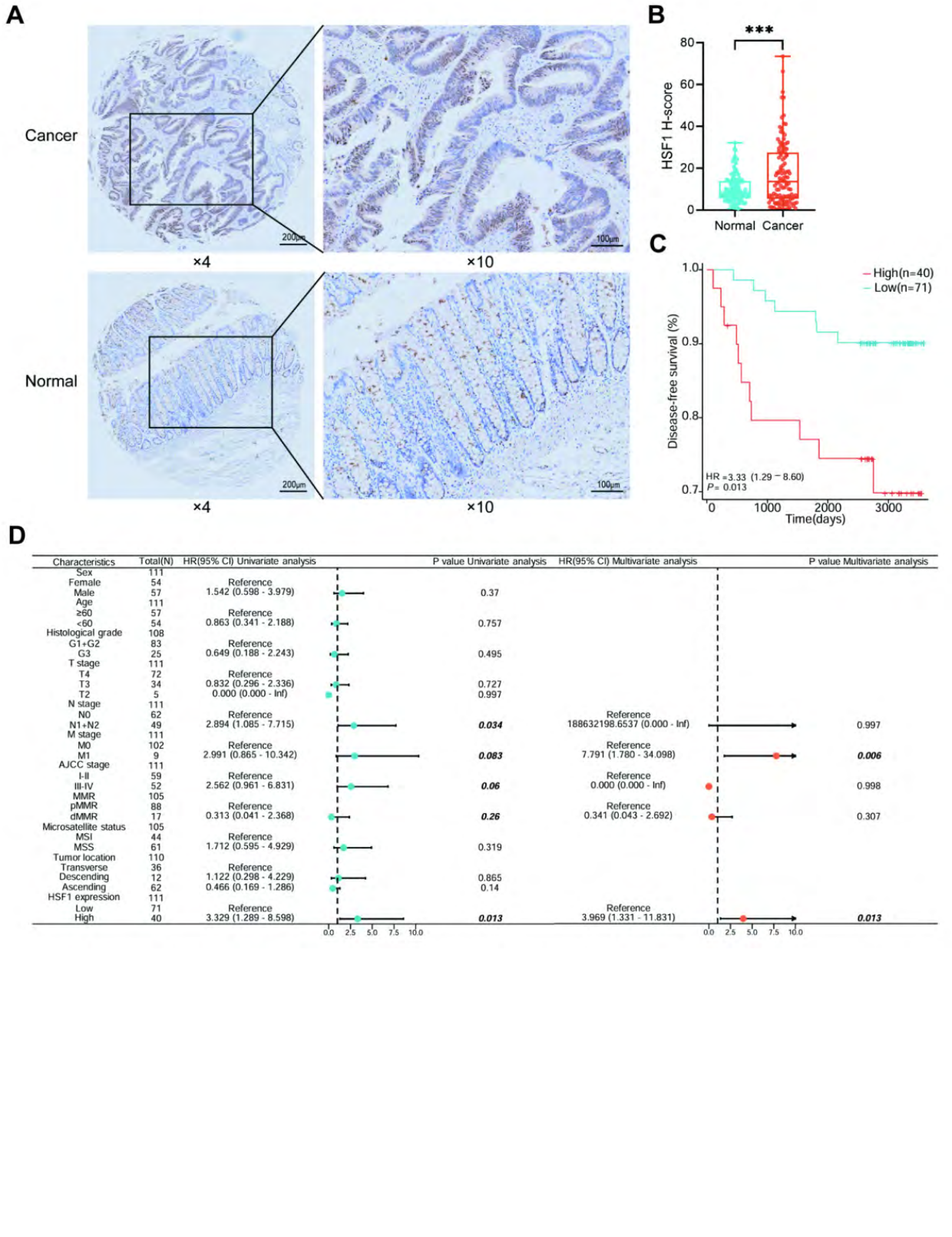

Fig. 3 [Download full resolution image]

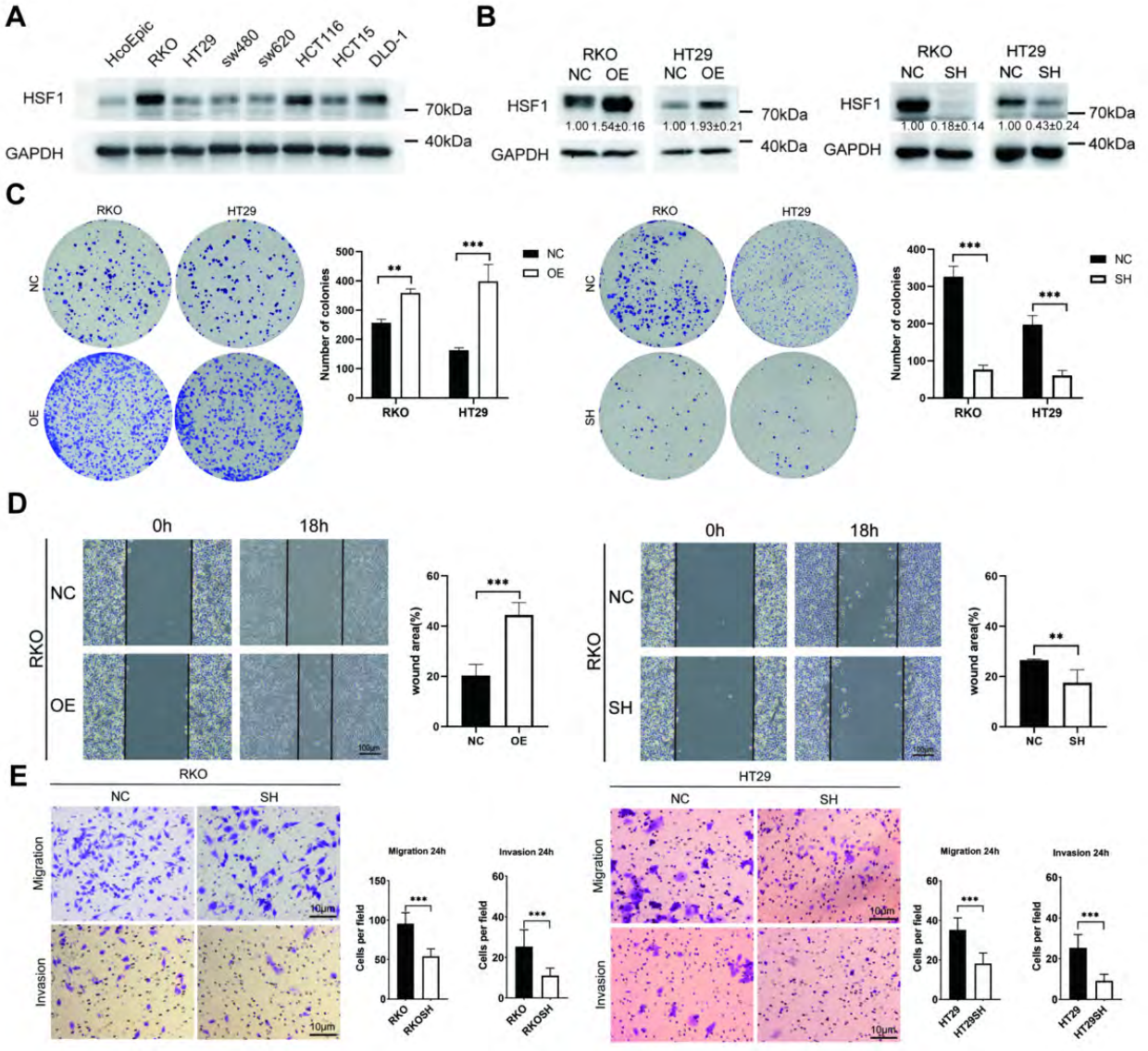

Fig. 4 Download full resolution image

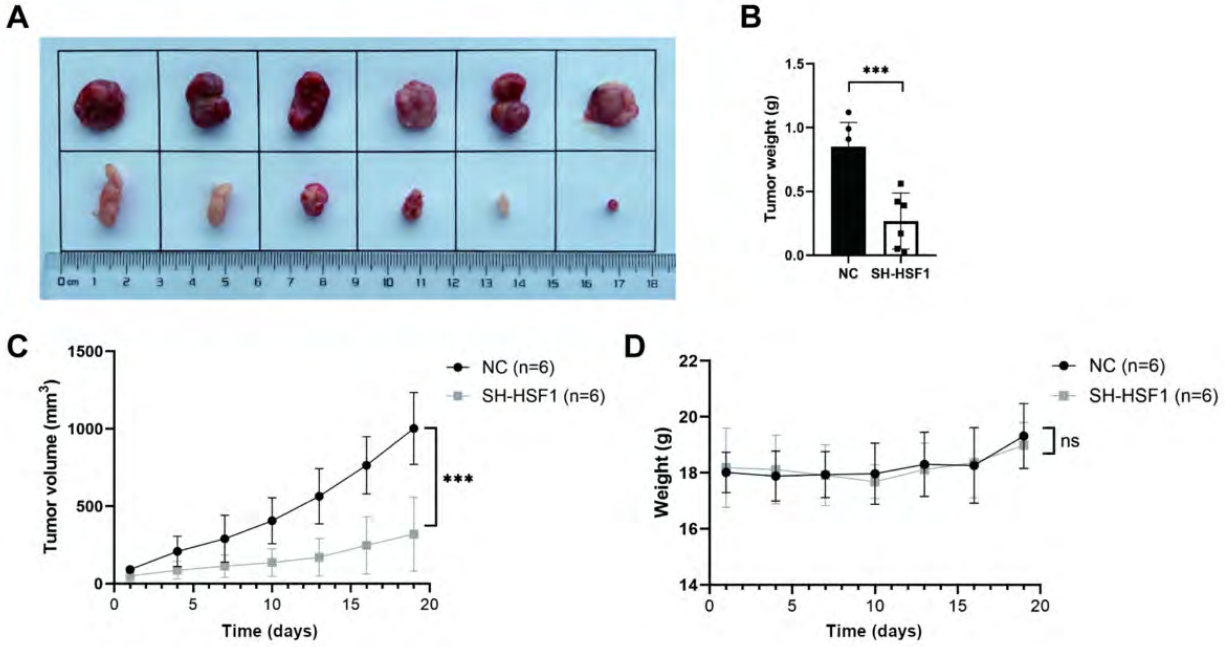

Fig. 5 [Download full resolution image]

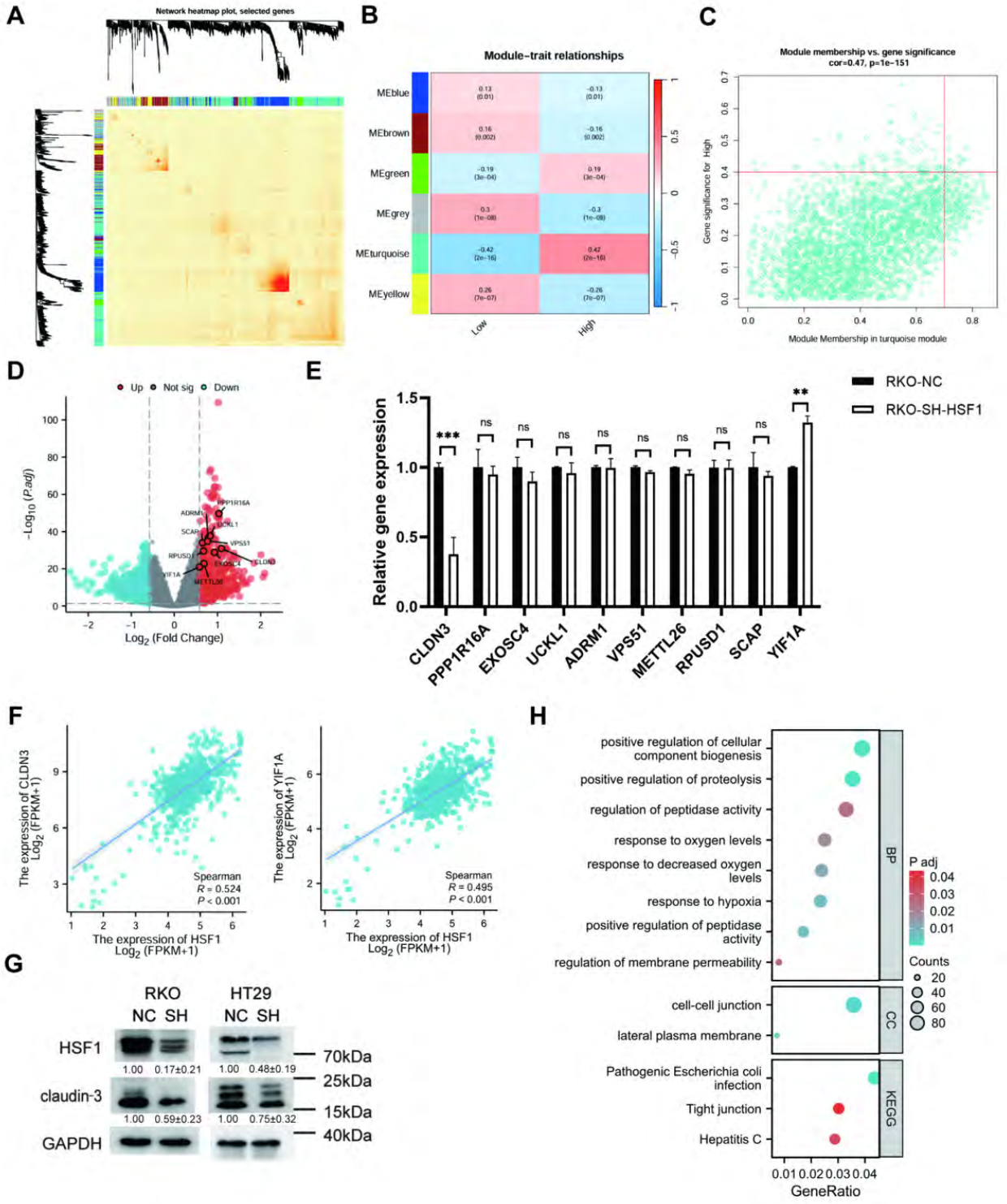

Fig. 6 [Download full resolution image]